

# Radiative Decays of the $\Upsilon(1S)$ to $\gamma\pi^0\pi^0$ , $\gamma\eta\eta$ and $\gamma\pi^0\eta$

D. Besson,<sup>1</sup> T. K. Pedlar,<sup>2</sup> D. Cronin-Hennessy,<sup>3</sup> K. Y. Gao,<sup>3</sup> D. T. Gong,<sup>3</sup> J. Hietala,<sup>3</sup> Y. Kubota,<sup>3</sup> T. Klein,<sup>3</sup> B. W. Lang,<sup>3</sup> R. Poling,<sup>3</sup> A. W. Scott,<sup>3</sup> A. Smith,<sup>3</sup> S. Dobbs,<sup>4</sup> Z. Metreveli,<sup>4</sup> K. K. Seth,<sup>4</sup> A. Tomaradze,<sup>4</sup> P. Zweber,<sup>4</sup> J. Ernst,<sup>5</sup> K. Arms,<sup>6</sup> H. Severini,<sup>7</sup> S. A. Dytman,<sup>8</sup> W. Love,<sup>8</sup> S. Mehrabyan,<sup>8</sup> J. A. Mueller,<sup>8</sup> V. Savinov,<sup>8</sup> Z. Li,<sup>9</sup> A. Lopez,<sup>9</sup> H. Mendez,<sup>9</sup> J. Ramirez,<sup>9</sup> G. S. Huang,<sup>10</sup> D. H. Miller,<sup>10</sup> V. Pavlunin,<sup>10</sup> B. Sanghi,<sup>10</sup> I. P. J. Shipsey,<sup>10</sup> G. S. Adams,<sup>11</sup> M. Anderson,<sup>11</sup> J. P. Cummings,<sup>11</sup> I. Danko,<sup>11</sup> J. Napolitano,<sup>11</sup> Q. He,<sup>12</sup> H. Muramatsu,<sup>12</sup> C. S. Park,<sup>12</sup> E. H. Thorndike,<sup>12</sup> T. E. Coan,<sup>13</sup> Y. S. Gao,<sup>13</sup> F. Liu,<sup>13</sup> M. Artuso,<sup>14</sup> C. Boulahouache,<sup>14</sup> S. Blusk,<sup>14</sup> J. Butt,<sup>14</sup> J. Li,<sup>14</sup> N. Menaa,<sup>14</sup> R. Mountain,<sup>14</sup> S. Nisar,<sup>14</sup> K. Randrianarivony,<sup>14</sup> R. Redjimi,<sup>14</sup> R. Sia,<sup>14</sup> T. Skwarnicki,<sup>14</sup> S. Stone,<sup>14</sup> J. C. Wang,<sup>14</sup> K. Zhang,<sup>14</sup> S. E. Csorna,<sup>15</sup> G. Bonvicini,<sup>16</sup> D. Cinabro,<sup>16</sup> M. Dubrovin,<sup>16</sup> A. Lincoln,<sup>16</sup> R. A. Briere,<sup>17</sup> G. P. Chen,<sup>17</sup> J. Chen,<sup>17</sup> T. Ferguson,<sup>17</sup> G. Tatishvili,<sup>17</sup> H. Vogel,<sup>17</sup> M. E. Watkins,<sup>17</sup> J. L. Rosner,<sup>18</sup> N. E. Adam,<sup>19</sup> J. P. Alexander,<sup>19</sup> K. Berkelman,<sup>19</sup> D. G. Cassel,<sup>19</sup> J. E. Duboscq,<sup>19</sup> K. M. Ecklund,<sup>19</sup> R. Ehrlich,<sup>19</sup> L. Fields,<sup>19</sup> R. S. Galik,<sup>19</sup> L. Gibbons,<sup>19</sup> R. Gray,<sup>19</sup> S. W. Gray,<sup>19</sup> D. L. Hartill,<sup>19</sup> B. K. Heltsley,<sup>19</sup> D. Hertz,<sup>19</sup> C. D. Jones,<sup>19</sup> J. Kandaswamy,<sup>19</sup> D. L. Kreinick,<sup>19</sup> V. E. Kuznetsov,<sup>19</sup> H. Mahlke-Krüger,<sup>19</sup> T. O. Meyer,<sup>19</sup> P. U. E. Onyisi,<sup>19</sup> J. R. Patterson,<sup>19</sup> D. Peterson,<sup>19</sup> E. A. Phillips,<sup>19</sup> J. Pivarski,<sup>19</sup> D. Riley,<sup>19</sup> A. Ryd,<sup>19</sup> A. J. Sadoff,<sup>19</sup> H. Schwarthoff,<sup>19</sup> X. Shi,<sup>19</sup> S. Stroiney,<sup>19</sup> W. M. Sun,<sup>19</sup> T. Wilksen,<sup>19</sup> M. Weinberger,<sup>19</sup> S. B. Athar,<sup>20</sup> P. Avery,<sup>20</sup> L. Breva-Newell,<sup>20</sup> R. Patel,<sup>20</sup> V. Potlia,<sup>20</sup> H. Stoeck,<sup>20</sup> J. Yelton,<sup>20</sup> P. Rubin,<sup>21</sup> C. Cawfield,<sup>22</sup> B. I. Eisenstein,<sup>22</sup> I. Karliner,<sup>22</sup> D. Kim,<sup>22</sup> N. Lowrey,<sup>22</sup> P. Naik,<sup>22</sup> C. Sedlack,<sup>22</sup> M. Selen,<sup>22</sup> E. J. White,<sup>22</sup> J. Wiss,<sup>22</sup> M. R. Shepherd,<sup>23</sup> D. M. Asner,<sup>24</sup> and K. W. Edwards<sup>24</sup>

(CLEO Collaboration)

<sup>1</sup>*University of Kansas, Lawrence, Kansas 66045*

<sup>2</sup>*Luther College, Decorah, Iowa 52101*

<sup>3</sup>*University of Minnesota, Minneapolis, Minnesota 55455*

<sup>4</sup>*Northwestern University, Evanston, Illinois 60208*

<sup>5</sup>*State University of New York at Albany, Albany, New York 12222*

<sup>6</sup>*Ohio State University, Columbus, Ohio 43210*

<sup>7</sup>*University of Oklahoma, Norman, Oklahoma 73019*

<sup>8</sup>*University of Pittsburgh, Pittsburgh, Pennsylvania 15260*

<sup>9</sup>*University of Puerto Rico, Mayaguez, Puerto Rico 00681*

<sup>10</sup>*Purdue University, West Lafayette, Indiana 47907*

<sup>11</sup>*Rensselaer Polytechnic Institute, Troy, New York 12180*

<sup>12</sup>*University of Rochester, Rochester, New York 14627*

<sup>13</sup>*Southern Methodist University, Dallas, Texas 75275*

<sup>14</sup>*Syracuse University, Syracuse, New York 13244*

<sup>15</sup>*Vanderbilt University, Nashville, Tennessee 37235*

<sup>16</sup>*Wayne State University, Detroit, Michigan 48202*

<sup>17</sup>*Carnegie Mellon University, Pittsburgh, Pennsylvania 15213*

<sup>18</sup>*Enrico Fermi Institute, University of Chicago, Chicago, Illinois 60637*

<sup>19</sup>*Cornell University, Ithaca, New York 14853*

<sup>20</sup>*University of Florida, Gainesville, Florida 32611*

<sup>21</sup>*George Mason University, Fairfax, Virginia 22030*

<sup>22</sup>*University of Illinois, Urbana-Champaign, Illinois 61801*

<sup>23</sup>*Indiana University, Bloomington, Indiana 47405*

<sup>24</sup>*Carleton University, Ottawa, Ontario, Canada K1S 5B6  
and the Institute of Particle Physics, Canada*

(Dated: November 28, 2005)

## Abstract

We report on a new study of exclusive radiative decays of the  $\Upsilon(1S)$  resonance into the final states  $\gamma\pi^0\pi^0$ ,  $\gamma\eta\eta$  and  $\gamma\pi^0\eta$ , using  $1.13\text{ fb}^{-1}$  of  $e^+e^-$  annihilation data collected at  $\sqrt{s} = 9.46\text{ GeV}$  with the CLEO III detector operating at the Cornell Electron Storage Ring. In the channel  $\gamma\pi^0\pi^0$ , we measure the branching ratio for the decay mode  $\Upsilon(1S) \rightarrow \gamma f_2(1270)$  to be  $(10.5 \pm 1.6\text{ (stat)} \pm 1.8\text{ (syst)}) \times 10^{-5}$ . We place upper limits on the product branching ratios for the isoscalar resonances  $f_0(1500)$  and  $f_0(1710)$  for the  $\pi^0\pi^0$  and  $\eta\eta$  decay channels. We also search for resonances decaying into  $\pi^0\eta$ . We find no evidence for any resonant structure and set an upper limit on the  $\Upsilon(1S)$  radiative decay into  $\pi^0\eta$ .

## I. INTRODUCTION

The present best estimates for the masses of glueballs come from lattice gauge theory calculations [1, 2]. They predict that the lightest glueball should have  $J^{PC} = 0^{++}$  and that its mass should be in the range of 1.45 to 1.75  $\text{GeV}/c^2$ . The scalar glueball is therefore expected to be too light to decay into a pair of vector mesons (e.g.,  $\omega\omega$ ,  $\rho\rho$ ,  $K^*\bar{K}^*$ ,  $\phi\phi$ ). Hence, a decay into two pseudo-scalars ( $J^{PC} = 0^{-+}$ ) is expected.

Unfortunately, the identification of a scalar glueball among the many established scalar resonances is rather difficult for two reasons. First, the scalar glueball has the same quantum numbers as a scalar meson ( $J^{PC} = 0^{++}$ ), and second, scalar meson resonances also prefer to decay into two pseudo-scalar mesons (e.g.,  $\pi\pi$ ,  $\eta\eta$ ,  $KK$ ) as would the scalar glueball. The possible mixing of the glueball with nearby scalar meson states further complicates the identification and classification of scalar states in the mass region between 1 and 2  $\text{GeV}/c^2$  [3]. Many of the lattice QCD models predict the decay ratios (e.g.,  $\eta\eta/\pi\pi$ ,  $\eta\eta/K\bar{K}$ , etc.) for a glueball and for scalar resonances [4], which provides a tool to distinguish between  $q\bar{q}$  mesons and exotic states. Hence, the measurement of these decay ratios is crucial to identify and establish a scalar resonance as a meson state, a glueball or a possible mixed gluonic-mesonic state.

In the last two decades, many hadron experiments have made precise measurements in the light meson region of 1 to 2  $\text{GeV}/c^2$ . Recently, the focus has been on the  $f_0$  triplet, comprising the  $f_0(1370)$ ,  $f_0(1500)$  and  $f_0(1710)$ . These resonances are candidates for the two  $1^3P_0(q\bar{q})$  states of the ground state scalar nonet ( $|u\bar{u}+d\bar{d}\rangle$  and  $|s\bar{s}\rangle$ ). This triplet clearly has a supernumerary character and could be a superposition of these quark states and a scalar glueball state. One place to search for the  $f_0$  triplet states is in radiative  $\Upsilon(1S)$  decays. In these decays, one of the three gluons from the quark-antiquark annihilation is replaced by a photon, which leaves two gluons to form a bound state (glue-rich environment). This environment is thought likely to produce glueballs or mixed gluonic-mesonic states rather than ordinary meson states. A similar environment is provided by radiative  $J/\psi$  decays, which were studied by the Crystal Ball, Mark III, DM2 and BES collaborations [9, 10, 11, 12, 13], leading to a list of two-body decay branching ratios. The establishment of a corresponding list for  $\Upsilon(1S)$  decays is therefore highly desirable and would not only deepen our understanding of  $c\bar{c}$  and  $b\bar{b}$  quarkonia, but could also contribute to the identification of a scalar glueball state or shed new light on its mixing with ordinary nearby meson states.

Radiative decays of the  $\Upsilon(1S)$  have been studied by many groups, including the ARGUS [14], DM1 [15] and CLEO collaborations. CLEO I found no obvious structure in the exclusive decay  $\Upsilon(1S) \rightarrow \gamma\pi\pi$  [16]. In CLEO II data, the first observation of a two-body  $\Upsilon(1S)$  decay, consistent with  $\Upsilon(1S) \rightarrow \gamma f_2(1270)$ , was made [17]. This measurement was repeated in a recent analysis by CLEO III of radiative  $\Upsilon(1S)$  decays into two charged pions [18] using a new data sample which has fifteen times higher statistics than the CLEO II data sample. The analysis included a confirmation of the spin of the  $f_2(1270)$  and a measurement of its helicity distribution. In this analysis, we use the same CLEO III  $\Upsilon(1S)$  data sample to study all-neutral decays of the  $f_2(1270)$  resonance and some members of the aforementioned  $f_0$  triplet into  $\pi^0$  and  $\eta$  final states.

## II. DETECTOR, DATA SAMPLE AND EVENT SELECTION

The analysis presented here uses data collected using the CLEO III detector configuration [19, 20, 21, 22, 23, 24, 25] at the Cornell Electron Storage Ring (CESR). The detector is equipped with a CsI(Tl) calorimeter, first installed in the CLEO II detector configuration, with an energy resolution matching that of the Crystal Ball (NaI(Tl) crystals) [26] and CUSB II (BGO crystals) [27] detectors. The finer segmentation of the CLEO calorimeter provides for better photon detection efficiency than the previous experiments. The CLEO III tracking detector, consisting of a silicon strip detector and a large drift chamber, provides improved suppression of backgrounds from charged particles. The magnetic field inside the tracking detector is 1.5 T.

We search for radiative  $\Upsilon(1S)$  decays in the modes  $\Upsilon(1S) \rightarrow \gamma\pi^0\pi^0$ ,  $\gamma\eta\eta$  and  $\gamma\pi^0\eta$ . The  $\Upsilon(1S)$  data ( $E_{cm} = 9.46$  GeV) sample consists of an integrated luminosity of  $1.13 \text{ fb}^{-1}$ , corresponding to  $(21.2 \pm 0.2(\text{syst})) \times 10^6$   $\Upsilon(1S)$  decays [28]. Continuum data with an integrated luminosity of  $192 \text{ pb}^{-1}$  were taken at  $E_{cm} \sim 9.43$  GeV, just below the  $\Upsilon(1S)$  resonance, and are used to study the continuum background under the  $\Upsilon(1S)$ .

Candidate events for the individual final states ( $\gamma\pi^0\pi^0$ ,  $\gamma\eta\eta$  and  $\gamma\pi^0\eta$ ) are selected in a similar fashion, using the following basic selection criteria. An event must have no charged tracks and exactly one electromagnetic shower in the barrel ( $|\cos\Theta| < 0.75$ , where  $\Theta$  represents the polar angle) or the endcap region ( $0.82 < |\cos\Theta| < 0.93$ ) of the calorimeter with an energy exceeding 4 GeV. There must be at least 4 other photons in the event, each with an energy greater than 10 MeV. All combinations of 2 photons in the event are then combined to form  $\pi^0$  and  $\eta$  candidates. To be selected an event must have 2 pairs of photons satisfying the requirement:

$$\sqrt{P_1^2(\pi_1^0/\eta_1) + P_2^2(\pi_2^0/\eta_2)} < 5,$$

with  $P_1$  and  $P_2$  being the pulls, defined as:

$$P(\pi^0/\eta) = [m_{\gamma\gamma} - m(\pi^0/\eta)] / \sigma_{\gamma\gamma},$$

where  $m_{\gamma\gamma}$  is the  $\gamma\gamma$  invariant mass,  $m(\pi^0/\eta)$  is the known  $\pi^0$  or  $\eta$  mass, and  $\sigma_{\gamma\gamma}$  is the expected  $\gamma\gamma$  mass resolution, which, in our case, has a typical value in the range of 5 - 7  $\text{MeV}/c^2$ .

To study the event-selection criteria and measure their efficiencies, we use a Monte Carlo simulation consisting of an event generator [29] and a GEANT-based [30] detector-response simulation. For each final state,  $\Upsilon(1S) \rightarrow \gamma X$  events are generated with  $X = f_2(1270)$ ,  $f_0(1500)$  and  $f_0(1710)$ , using a symmetric Breit-Wigner line-shape and the PDG mass and width [31] listed in Table I. The recoiling  $X$  system is then forced to decay to  $\pi^0\pi^0$  or  $\eta\eta$ , and propagated through the detector. A fit to the invariant  $\pi^0\pi^0$  and  $\eta\eta$  mass spectra after the basic selection cuts reveals significant differences in the mass and width values from the ones used at the generator level. In particular, we observe a shift of the mass and an increase of the width for each resonance. Table I lists the values of the generated and reconstructed resonance parameters.

The mass shifts are artifacts of the shower reconstruction in the calorimeter of such fast  $\pi^0$  and  $\eta$  mesons. Typical momenta of the  $\pi^0$  and  $\eta$  candidates in our samples are in the range 2 - 4 GeV. At these momenta, the two showers from a  $\pi^0$  or  $\eta$  will tend to overlap considerably in the CLEO calorimeter, which frequently results in an incorrect attribution

Resonance	Generated	Mass / Width in $\text{MeV}/c^2$	
		Reconstructed ( $\pi^0\pi^0$ )	Reconstructed ( $\eta\eta$ )
$f_2(1270)$	1275 / 185	$1255.4 \pm 1.6 / 199.9 \pm 4.7$	$1267.0 \pm 2.2 / 191.5 \pm 8.5$
$f_0(1500)$	1507 / 109	$1488.2 \pm 0.8 / 134.1 \pm 2.1$	$1501.5 \pm 1.1 / 124.2 \pm 2.9$
$f_0(1710)$	1713 / 125	$1692.6 \pm 1.2 / 151.2 \pm 4.9$	$1703.0 \pm 1.8 / 151.8 \pm 6.7$

TABLE I: Monte Carlo generated and reconstructed masses and widths of the three intermediate resonances  $f_2(1270)$ ,  $f_0(1500)$  and  $f_0(1710)$  after the basic selection cuts for the final states  $\gamma\pi^0\pi^0$  and  $\gamma\eta\eta$ . The errors shown are statistical only.

of too much energy to the softer of the two showers. This, in turn, causes the opening angle between the two showers to be underestimated. Although each pair of showers is then subject to a kinematic fit to the parent hypothesis, which will correct some of the fluctuations, a bias in the  $f_J$  resonance mass of 1 - 2% remains. We choose to perform our fits to these shifted distributions using Monte Carlo events as a guide to expected shapes rather than attempting to correct individual event masses. The increase in the widths can be attributed to the detector energy resolution and is consistent with the known mass resolution of about 50  $\text{MeV}/c^2$ . For the measurement of the  $f_2(1270)$  branching ratio, as well as for all upper limit branching ratio measurements, we use the mass and width values determined from the Monte Carlo study.

In addition to the basic selection criteria described above, a 4-momentum cut and an asymmetry cut are used to further select candidate events. Ideally, all reconstructed events should have the 4-momentum of the center-of-mass system, and one expects a Gaussian distribution around the center of the 4-momentum value. In reality, this is not the case and events differ from the center-of-mass 4-momentum due to the mis-reconstruction of the particles' energies or angles. For the  $\gamma\pi^0\pi^0$  final state selection, the allowed region for the 4-momentum is bounded by the following three conditions:

$$\begin{aligned} |\vec{p}| &= -0.30 - 1.20 \Delta E, \\ |\vec{p}| &= 0.25 - 0.80 \Delta E, \\ |\vec{p}| &= 1.10 + 0.50 \Delta E, \end{aligned}$$

where  $\Delta E$  is the difference between the reconstructed event energy and the center-of-mass energy ( $E_{\text{cm}}$ ) in GeV and  $|\vec{p}|$  is the magnitude of the reconstructed total event momentum in  $\text{GeV}/c$ . These cuts include the  $\Delta E - |\vec{p}|$  area where the 4-momentum is conserved for the entire event and, in addition, the region where the single, recoiling photon loses energy. For the latter, the 4-momentum is not conserved for the entire event but only for the intermediate resonance  $X$  in the decay chain  $\Upsilon(1S) \rightarrow \gamma X \rightarrow \gamma\pi^0\pi^0$ . Figure 1 illustrates the chosen 4-momentum region with a sample of 40,000 Monte Carlo events of the type  $\Upsilon(1S) \rightarrow \gamma f_2(1270) \rightarrow \gamma\pi^0\pi^0$ , after the basic selection cuts are applied.

Similarly, we define the 4-momentum allowed region for the  $\gamma\eta\eta$  final state selection as follows:

$$\begin{aligned} |\vec{p}| &= -0.25 - 1.20 \Delta E, \\ |\vec{p}| &= 0.25 - 0.65 \Delta E, \\ |\vec{p}| &= 0.85 + 0.50 \Delta E, \end{aligned}$$

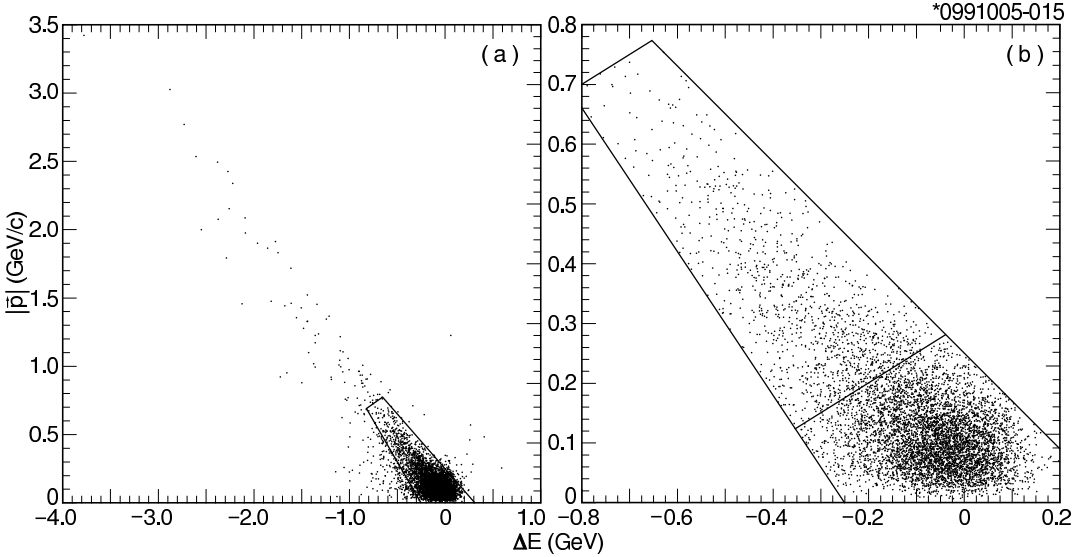


FIG. 1: Illustration of the chosen 4-momentum distribution cuts on a larger (a) and smaller (b) scale, using Monte Carlo events for the decay channel  $\Upsilon(1S) \rightarrow \gamma f_2(1270) \rightarrow \gamma\pi^0\pi^0$ . The slanted line in the lower right part of (b) divides the selected events roughly into two categories: the lower area where the 4-momentum is conserved for the entire event; the upper area where the 4-momentum is conserved for the intermediate resonance but not for the entire event. The remaining events outside the selected area in (a) have an energy loss from more than one photon and, hence, are excluded from the selection.

with  $\Delta E$  and  $|\vec{p}|$  as described above. Figure 2 illustrates the chosen 4-momentum region with a sample of 40,000 Monte Carlo events of the type  $\Upsilon(1S) \rightarrow \gamma f_2(1270) \rightarrow \gamma\eta\eta$ , after the basic selection cuts are applied.

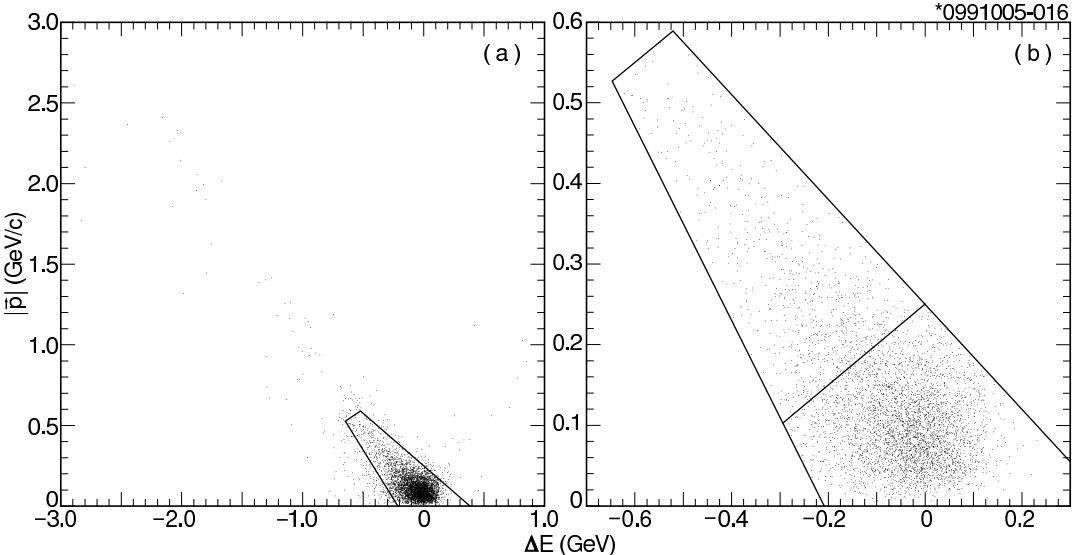


FIG. 2: Similar to Figure 1, but for the decay channel  $\Upsilon(1S) \rightarrow \gamma f_2(1270) \rightarrow \gamma\eta\eta$ .

A source of background originates from combining a wrong pair of photons to form a  $\pi^0$

or  $\eta$  candidate. Usually,  $\pi^0$  and  $\eta$  mesons decay isotropically and their angular distributions are flat. However, the  $\pi^0$  and  $\eta$  candidates which originate from a wrong photon combination do not have a flat angle distribution and, hence, can be removed by a cut which utilizes the polar  $\Delta\varphi$  and azimuthal  $\Delta\Theta$  angle differences between the two photons from a decay candidate. We refer to this cut as an asymmetry cut since it is equivalent to a traditional cut using the energy asymmetry  $[E(\gamma_1) - E(\gamma_2)]/[E(\gamma_1) + E(\gamma_2)]$  of the two photons from the  $\pi^0$  or  $\eta$ . For the  $\gamma\pi^0\pi^0$  final state the asymmetry cut is defined as  $\sqrt{\Delta\Theta^2 + \Delta\varphi^2} < 40^\circ$ , while for the  $\gamma\eta\eta$  final state the cut is  $\sqrt{\Delta\Theta^2 + \Delta\varphi^2} < 60^\circ$ .

Since we are interested in measuring the branching ratios for the isoscalar resonances  $f_2(1270)$ ,  $f_0(1500)$  and  $f_0(1710)$ , it is not necessary to determine the selection efficiency over an entire mass range, but sufficient to determine it for each of the resonances individually. The final event selection efficiencies, after the basic and extended selection cuts, are summarized in Table II. The uncertainties shown are statistical only. The largest drop in the reconstruction efficiency is from the requirement on the pulls of the 2  $\gamma\gamma$  mass combinations.

Resonance	Reconstruction Efficiency in %	
	$\gamma\pi^0\pi^0$	$\gamma\eta\eta$
$f_2(1270)$	$16.4 \pm 0.2$	$10.2 \pm 0.2$
$f_0(1500)$	$20.4 \pm 0.3$	$9.1 \pm 0.2$
$f_0(1710)$	$20.6 \pm 0.3$	$8.6 \pm 0.2$

TABLE II: Reconstruction efficiencies for various intermediate resonances in the  $\gamma\pi^0\pi^0$  and  $\gamma\eta\eta$  final states after the extended selection cuts are applied.

Contrary to the analysis in [18], the process  $e^+e^- \rightarrow \gamma\rho$  does not contribute to the background in our analysis. The major background contribution rather originates from non-resonant continuum processes. Ideally, one could account for this source of background by performing a continuum subtraction. Unfortunately, our  $\Upsilon(1S)$  continuum data sample is too small. No events remain after applying the extended selection cuts for the  $\gamma\pi^0\pi^0$  and the  $\gamma\eta\eta$  final states. Hence, we use a parametrization of the continuum background derived from a Monte Carlo simulation. We use 38 million generically generated continuum Monte Carlo events, which corresponds to an integrated luminosity of  $13.5 \text{ fb}^{-1}$ .

After applying all the selection criteria, we fit the resulting  $\pi^0\pi^0$  invariant mass distribution to a threshold function which has the following form:

$$F(x) = N \cdot (x - T) \cdot e^{c_1(x - T) + c_2(x - T)^2}$$

where  $x$  is the  $\pi^0\pi^0$  invariant mass,  $N$  is a scale factor,  $T = 0.28 \text{ GeV}/c^2$  (the minimum  $\pi^0\pi^0$  invariant mass) and  $c_1$ ,  $c_2$  are free parameters. The fit is shown in Figure 3.

Since only 2 Monte Carlo continuum events remain for the  $\gamma\eta\eta$  final state after all the extended selection cuts, we do not perform a similar parametrization but assume the continuum background for this channel is negligible.

### III. ANALYSIS AND RESULTS

Figure 4 shows the  $\pi^0\pi^0$  and  $\eta\eta$  invariant mass plots after the final selection. As can be clearly seen in Figure 4(a), the  $\pi^0\pi^0$  invariant mass distribution is dominated by the

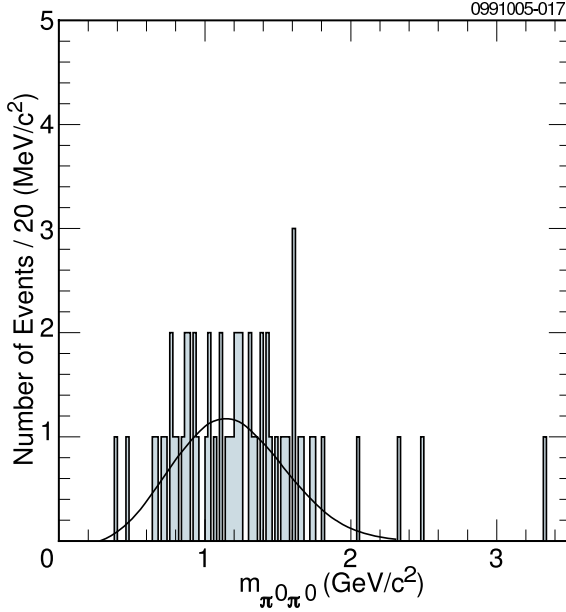


FIG. 3: The  $\pi^0\pi^0$  invariant mass distribution from generic continuum ( $E_{\text{cm}} = 10.54$  GeV) Monte Carlo events for the final state  $\gamma\pi^0\pi^0$  after the extended selection cuts, with the fit of the threshold function overlaid.

isoscalar resonance  $f_2(1270)$ . The  $\eta\eta$  invariant mass distribution, Figure 4(b), has only two events, which is too few to show any resonant structure.

The Monte Carlo signal events for the processes  $\Upsilon(1S) \rightarrow \gamma X \rightarrow \gamma\pi^0\pi^0/\eta\eta$  are produced with a decay angle distribution which is characteristic of the spin of the final state (i.e.  $J = 0$  for  $f_0(1500)$  and  $J = 2$  for  $f_2(1270)$ ). However, the generation does not take into account the correct helicity distribution for the  $f_2(1270)$  since this distribution depends on the specific decay channel and can only be determined from the data itself. The efficiencies for the various intermediate states in Table II are based on studies using Monte Carlo signal events without the correct helicity distribution and, hence, have to be adjusted for this. The method to obtain the correct helicity-angle distributions is described in detail in [18] and results in a helicity correction factor which takes into account decay-dependent efficiency corrections and the helicity substructure for the final state resonance. We use the same approach in our analysis, but for the determination of the helicity correction factor for the  $f_2(1270)$  we replace our measured helicity substructure with the more precise one from [18]. This is legitimate since the substructure is independent of the decay into  $\pi^0\pi^0$  or  $\pi^+\pi^-$ . With this method we obtain a correction factor for the  $f_2(1270)$  of  $0.66 \pm 0.04$ , where the error is statistical only. This factor multiplies the efficiency stated in Table II.

### A. Exclusive Radiative Decay $\Upsilon(1S) \rightarrow \gamma\pi^0\pi^0$

To determine the branching ratio for  $\Upsilon(1S) \rightarrow \gamma f_2(1270)$ , we fit the invariant  $\pi^0\pi^0$  mass distribution with a spin-dependent Breit-Wigner line-shape of fixed mass and width, as described in [18]. The values determined from Monte Carlo studies shown in Table I were used. Although these mass and width values were determined using a symmetric Breit-Wigner line-shape for the Monte Carlo generation and fit, the observed masses and widths can still be

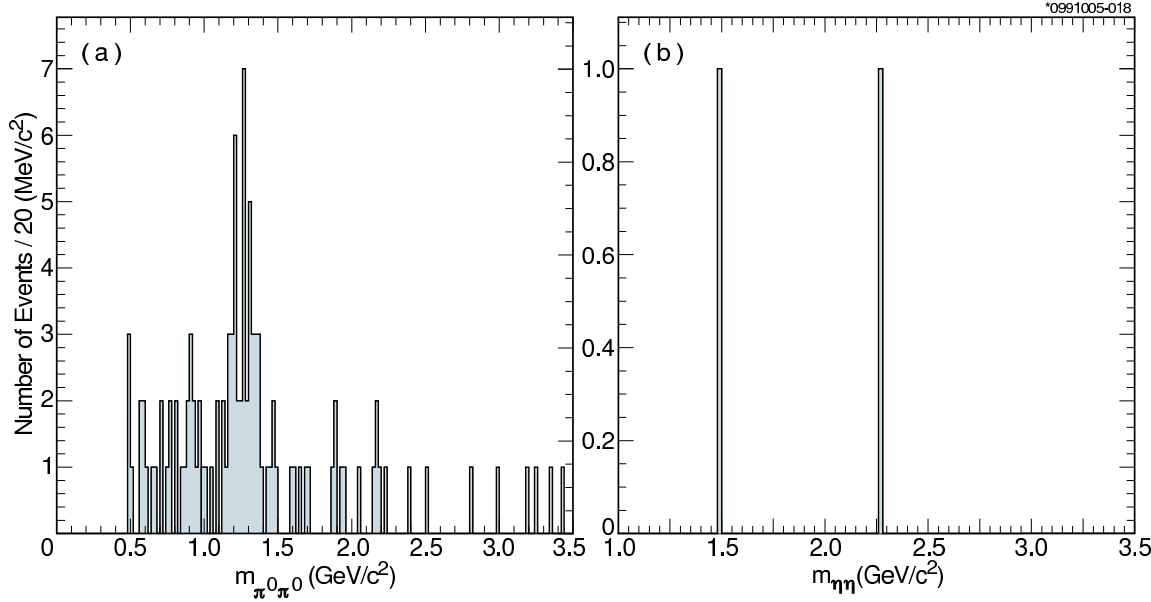


FIG. 4: The (a)  $\pi^0\pi^0$  and (b)  $\eta\eta$  invariant mass distributions from the  $\Upsilon(1S)$  data sample after the extended selection cuts. These distributions are not corrected for continuum background or reconstruction efficiency.

used in a spin-dependent Breit-Wigner line-shape fit, because the systematic uncertainty introduced by using the symmetric line-shape can be directly translated into a systematic uncertainty emerging from the width increase. To account for the continuum background, the threshold parametrization function described previously was applied. Figure 5 shows the invariant  $\pi^0\pi^0$  mass distribution and the results of the fit using the Breit-Wigner line-shape and the background parametrization function. Integrating the Breit-Wigner line-shape fit from 0.28 to 3.0  $\text{GeV}/c^2$ , gives  $67.7 \pm 9.5$  events for the  $f_2(1270)$ . This number of events is larger than the number of events in the peak of the invariant mass distribution since we integrate the line-shape over the entire mass range from 0.28 to 3.0  $\text{GeV}/c^2$ .

When extending the fit interval to include such a large range, it is legitimate to question the influence of other resonances in this mass range, although they may not be visible in the distribution. We do not rule out possible contributions of higher mass resonances to the mass distribution. Unfortunately, any inclusion of further resonances in the fit is limited by the small number of events in that mass range. In determining upper limits for other resonances, all other parameters in the fit are fixed to their previous values and only one extra resonance is introduced at a time. Since no visible contributions of additional resonances can be seen in the invariant mass distribution, we consider their influence as negligible for the  $f_2(1270)$  results.

With the results from the above line-shape fit, the efficiency from Table II and the helicity-correction factor, we determine the product branching ratio for the  $f_2(1270)$  to be:

$$\mathcal{B}(\Upsilon(1S) \rightarrow \gamma f_2(1270)) \cdot \mathcal{B}(f_2(1270) \rightarrow \pi^0\pi^0) = (3.0 \pm 0.5) \times 10^{-5},$$

where the error is statistical only.

We determine a systematic error on this branching ratio of  $\pm 17\%$ . The largest contribution to this error originates from uncertainties in the line-shape fit and the thresh-

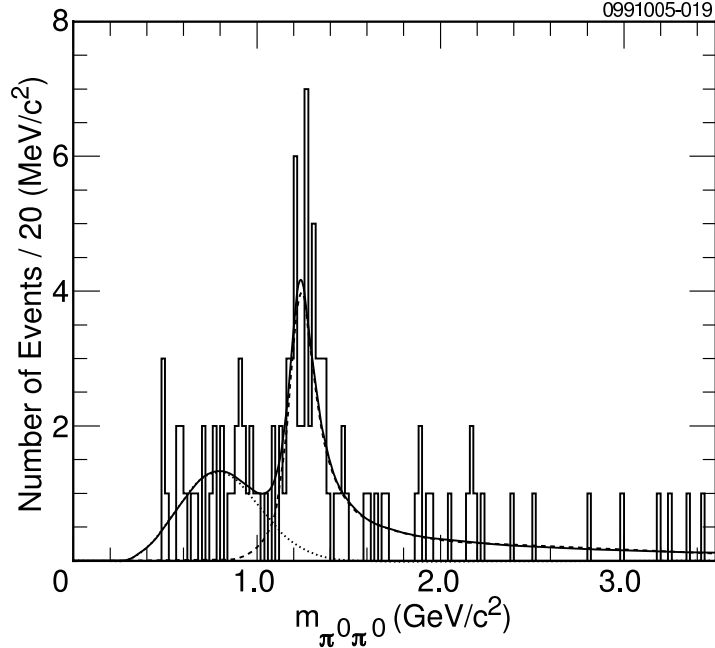


FIG. 5: The  $\pi^0\pi^0$  invariant mass distribution from the  $\Upsilon(1S)$  data sample after the extended selection cuts. The solid line shows the combined fit to a spin-dependent Breit-Wigner line-shape and a threshold function to account for the continuum background and threshold effects. In addition, the threshold function (dotted line) and Breit-Wigner (dashed line) contributions are shown separately.

old function used for the background parametrization. Other contributions include systematic uncertainties from the mass shift,  $\pi^0$  reconstruction and extended selection cuts. Taking into account the isoscalar nature of the  $f_2(1270)$  and the branching ratio of  $\mathcal{B}(f_2(1270) \rightarrow \pi\pi) = 0.847^{+0.024}_{-0.013}$  [31], we determine an overall  $\Upsilon(1S)$  radiative decay branching ratio to  $f_2(1270)$  of:

$$\mathcal{B}(\Upsilon(1S) \rightarrow \gamma f_2(1270)) = (10.5 \pm 1.6 \text{ (stat)} \pm 1.8 \text{ (syst)}) \times 10^{-5}.$$

To set upper limits on the branching ratios for other likely resonances in the  $\gamma\pi^0\pi^0$  final state, we include an additional spin-dependent Breit-Wigner line-shape in the  $f_2(1270)$  branching ratio fit, with values for the mass and width determined from our Monte Carlo studies. We fix the area of the additional Breit-Wigner and then repeat the fit using different values for the number of events. We then plot the number of events versus their likelihood from the fit, numerically integrate the area under the curve and determine the number of events where 90% of the area is covered. This number represents the upper limit at the 90% confidence level (C.L.).

With the above described method, we determine the number of events at the 90% C.L. upper limit for the  $f_0(1500)$  to be  $4.86 \pm 0.05$  and for the  $f_0(1710)$  to be  $4.41 \pm 0.05$ , where the errors are the systematic uncertainty from the integration process. Using similar methods as with the  $f_2(1270)$ , we find the systematic uncertainties on the  $f_0(1500)$  and  $f_0(1710)$  branching ratios to be  $^{+6.4\%}_{-5.7\%}$  and  $^{+6.6\%}_{-5.9\%}$ , respectively. Combining the statistical and systematic errors in quadrature and using the branching ratio  $\mathcal{B}(f_0(1500) \rightarrow \pi\pi) = 0.349 \pm 0.023$  [31], we determine the 90% C.L. upper limit branching ratio for the  $f_0(1500)$

to be:

$$\mathcal{B}(\Upsilon(1S) \rightarrow \gamma f_0(1500)) < 1.17 \times 10^{-5},$$

and the product branching ratio for the  $f_0(1710)$  to be:

$$\mathcal{B}(\Upsilon(1S) \rightarrow \gamma f_0(1710)) \cdot \mathcal{B}(f_0(1710) \rightarrow \pi^0 \pi^0) < 1.2 \times 10^{-6}.$$

### B. Exclusive Radiative Decay $\Upsilon(1S) \rightarrow \gamma \eta \eta$

We see no evidence for any resonant structure in the invariant  $\eta \eta$  mass distribution after the extended selection, or even after the basic selection. Hence, we measure upper limit branching ratios for the  $f_0(1500)$  and  $f_0(1710)$ . For this determination we use the simple method of event counting. The final invariant mass plot has negligible background and, hence, we assume all events are from the  $\Upsilon(1S) \rightarrow \gamma \eta \eta$  final state. Therefore, the number of events follows a Poisson distribution. For the  $f_0(1500)$  we find 1 event in the mass interval of 1 full-width around its mass and 0 events for the  $f_0(1710)$ , which translates into 90% C.L. upper limits of 3.9 and 2.3 events, respectively.

The systematic uncertainty for the  $f_0(1500)$  and the  $f_0(1710)$  is  $^{+31\%}_{-14\%}$ . The largest contributions to these uncertainties originate from the extended selection criteria (4-momentum,  $\eta$  asymmetry) which are on the order of 20%. Combining the statistical and systematical uncertainties, we determine the 90% C.L. upper limit on the product branching ratio for the  $f_0(1500)$  to be:

$$\mathcal{B}(\Upsilon(1S) \rightarrow \gamma f_0(1500)) \cdot \mathcal{B}(f_0(1500) \rightarrow \eta \eta) < 3.0 \times 10^{-6},$$

and for the  $f_0(1710)$  to be:

$$\mathcal{B}(\Upsilon(1S) \rightarrow \gamma f_0(1710)) \cdot \mathcal{B}(f_0(1710) \rightarrow \eta \eta) < 1.9 \times 10^{-6}.$$

### C. Exclusive Radiative Decay $\Upsilon(1S) \rightarrow \gamma \pi^0 \eta$

In the decay  $\Upsilon(1S) \rightarrow \gamma X$ , if the intermediate resonance  $X$  is a  $q\bar{q}$  meson state, it can only decay into a pair of pseudo-scalars ( $J^P = 0^-$ ) with  $I = 0$ , e.g.  $\eta\eta$ , or  $I = 1$ , e.g.  $\pi\pi$ . If  $X$  is an exotic state, i.e. a glueball or hybrid, it can also decay to the  $\pi^0\eta$  final state. We have searched for such a decay. After the same basic cuts were applied to the  $\Upsilon(1S)$  data sample as for the previous analyses, we find 3 events, with no events remaining after applying the 4-momentum cut used for the  $\gamma\pi^0\pi^0$  selection and the asymmetry cut used for the  $\gamma\eta\eta$  selection. Hence, we determine an upper limit for the branching ratio  $\Upsilon(1S) \rightarrow \gamma\pi^0\eta$ .

We use the same method as for the upper limit determination in the  $\Upsilon(1S) \rightarrow \gamma\eta\eta$  final state. To measure the reconstruction efficiency for any exotic-state mass, we generate Monte Carlo events of the type  $\Upsilon(1S) \rightarrow \gamma\pi^0\eta$  with a flat  $\pi^0\eta$  invariant mass distribution between 0.7 and 3  $\text{GeV}/c^2$ , and use the lowest efficiency found in the entire mass distribution of  $(4.8 \pm 0.5)\%$ .

Having no events in the data over the mass range of 0.7 to 3.0  $\text{GeV}/c^2$  corresponds to a 90% C.L. upper limit of 2.3 events. Combining this with a systematic error of  $^{+24\%}_{-14\%}$ , due to the same sources of uncertainty as with the previous 2 analyses, we determine the 90% C.L. upper limit for the branching ratio to be:

$$\mathcal{B}(\Upsilon(1S) \rightarrow \gamma\pi^0\eta) < 2.8 \times 10^{-6}.$$

## IV. SUMMARY AND CONCLUSIONS

We have analyzed  $1.13 \text{ fb}^{-1}$  of data from the CLEO III detector at the  $\Upsilon(1S)$  for resonances in the radiative decay channels  $\Upsilon(1S) \rightarrow \gamma\pi^0\pi^0$ ,  $\gamma\eta\eta$  and  $\gamma\pi^0\eta$ .

In the decay channel  $\gamma\pi^0\pi^0$ , we measure a branching ratio value for the isoscalar resonance  $f_2(1270)$  of  $\mathcal{B}(\Upsilon(1S) \rightarrow \gamma f_2(1270)) = (10.5 \pm 1.6 \pm 1.8) \times 10^{-5}$ . This is in excellent agreement with the same branching ratio obtained from the charged final state  $\gamma\pi^-\pi^+$ , using the same CLEO III data sets:  $\mathcal{B}(\Upsilon(1S) \rightarrow \gamma f_2(1270)) = (10.2 \pm 0.8 \pm 0.7) \times 10^{-5}$  [18]. Our result also agrees within the uncertainties with the earlier CLEO II measurement of  $(8.1 \pm 2.3 \pm 2.7) \times 10^{-5}$ , based on the decay channel  $\gamma\pi^-\pi^+$  [17]. One reason for the variation in the central values in this case is the helicity-correction factor for the efficiency that we employed, but which was missing in the earlier CLEO II measurement due to the limited statistics.

In addition, we determine 90% C.L. upper limits for the isoscalar resonances  $f_0(1500)$  and  $f_0(1710)$  decaying into  $\pi\pi$ , as well as a 90% C.L. upper limit for the decay  $\Upsilon(1S) \rightarrow \gamma f_0(1500)$ . We find that the upper limit branching ratio for the radiative decay into the  $f_0(1500)$  is almost an order of magnitude smaller than the branching ratio for the decay into the  $f_2(1270)$ . Based on the scalar-glueball mixing matrix from [4], QCD factorization model calculations in [32] predict branching ratios for the  $f_0(1500)$  and  $f_0(1710)$  to be  $\mathcal{B}(\Upsilon(1S) \rightarrow \gamma f_0(1500)) \approx 42 - 84 \times 10^{-5}$  and  $\mathcal{B}(\Upsilon(1S) \rightarrow \gamma f_0(1710)) \cdot \mathcal{B}(f_0(1710) \rightarrow \pi^0\pi^0) \approx 6 - 12 \times 10^{-6}$ . Our measurements of  $\mathcal{B}(\Upsilon(1S) \rightarrow \gamma f_0(1500)) < 1.17 \times 10^{-5}$  and  $\mathcal{B}(\Upsilon(1S) \rightarrow \gamma f_0(1710)) \cdot \mathcal{B}(f_0(1710) \rightarrow \pi^0\pi^0) < 1.2 \times 10^{-6}$  disagree with these predictions by more than an order of magnitude.

We do not attempt to determine a 90% C.L. upper limit for the decay  $\Upsilon(1S) \rightarrow \gamma f_0(1370)$ , since the mass region of the  $f_0(1370)$  overlaps to a large extent with the  $f_2(1270)$  region and the limited statistics do not allow for a fit with two line-shapes in the same mass region.

In the  $\gamma\eta\eta$  decay channel, no resonant structures are observed. This is consistent with what we would expect, given the size of our data sample, our reconstruction efficiency and the production of a resonance with a relatively large branching ratio decaying into  $\eta\eta$ , i.e.  $f_2(1270)$ . Therefore, we determine a 90% C.L. upper limit on the branching ratios for the isoscalar resonances  $f_0(1500)$  and  $f_0(1710)$  decaying into  $\eta\eta$  to  $\mathcal{B}(\Upsilon(1S) \rightarrow \gamma f_0(1500)) \cdot \mathcal{B}(f_0(1500) \rightarrow \eta\eta) < 3.0 \times 10^{-6}$  and  $\mathcal{B}(\Upsilon(1S) \rightarrow \gamma f_0(1710)) \cdot \mathcal{B}(f_0(1710) \rightarrow \eta\eta) < 1.9 \times 10^{-6}$ .

The search for exotic states in the  $\gamma\pi^0\eta$  decay channel does not show any evidence of states with exotic quantum numbers. We determine a 90% C.L. upper limit on the branching ratio for the decay  $\Upsilon(1S) \rightarrow \gamma\pi^0\eta$  for any intermediate state with a mass between 0.7 and 3.0  $\text{GeV}/c^2$  to  $\mathcal{B}(\Upsilon(1S) \rightarrow \gamma\pi^0\eta) < 2.8 \times 10^{-6}$ .

We gratefully acknowledge the effort of the CESR staff in providing us with excellent luminosity and running conditions. A. Ryd thanks the A.P. Sloan Foundation. This work was supported by the National Science Foundation and the U.S. Department of Energy.

---

- [1] C.J. Morningstar *et al.*, Phys. Rev. **D60** (1999) 034509.
- [2] C.J. Morningstar *et al.*, AIP Conf. Proc. **688** (2004) 220.
- [3] F.E. Close and A. Kirk, Phys. Lett. **B483** (2000) 345.
- [4] F.E. Close and A. Kirk, Eur. Phys. J. **C21** (2001) 531.

- [5] V.V. Anisovich *et al.* (Crystal Barrel Collaboration), Phys. Lett. **B323** (1994) 233.
- [6] C. Amsler *et al.* (Crystal Barrel Collaboration), Phys. Lett. **B333** (1994) 277.
- [7] C. Amsler *et al.* (Crystal Barrel Collaboration), Phys. Lett. **B342** (1995) 433.
- [8] D. Barberis *et al.* (WA102 Collaboration), Phys. Lett. **B479** (2000) 59.
- [9] J.E. Augustin *et al.* (DM2 Collaboration), Z. Phy. **C36** (1987) 369.
- [10] R.M. Baltrusaitis *et al.* (Mark III Collaboration), Phys. Rev. **D35** (1987) 2077.
- [11] C. Edwards *et al.* (Crystal Ball Collaboration), Phys. Rev. Lett. **48** (1982) 458.
- [12] J.Z. Bai *et al.* (BES Collaboration), Phys. Rev. Lett. **81** (1998) 1179.
- [13] X.Y. Shen *et al.* (BES Collaboration), Proceedings of Physics in Collision 2002, eConf **C020620:THAT07** (2002).
- [14] H. Albrecht *et al.* (ARGUS Collaboration), Z. Phy. **C42** (1989) 349.
- [15] S. Bary *et al.* (DM1 Collaboration), Phys. Rep. **267** (1996) 71.
- [16] R. Fulton *et al.* (CLEO Collaboration), Phys. Rev. **D41** (1990) 1401.
- [17] A. Anastassov *et al.* (CLEO Collaboration), Phys. Rev. Lett. **82** (1999) 286.
- [18] S.B. Athar *et al.* (CLEO Collaboration), hep-ex/0510015 (2005), submitted to Phys. Rev. D.
- [19] Y. Kubota *et al.* (CLEO Collaboration), Nucl. Inst. Meth. **A320** (1992) 66.
- [20] S. Koop *et al.* (CLEO Collaboration), Nucl. Inst. Meth. **A384** (1996) 61.
- [21] A. Wolf *et al.* (CLEO Collaboration), Nucl. Inst. Meth. **A408** (1998) 58.
- [22] G. Viehhauser *et al.*, Nucl. Inst. Meth. **A462** (2001) 146.
- [23] D. Peterson *et al.*, Nucl. Inst. Meth. **A478** (2002) 142.
- [24] A. Warburton *et al.*, Nucl. Inst. Meth. **A488** (2002) 451.
- [25] M. Artuso *et al.*, Nucl. Inst. Meth. **A502** (2003) 91.
- [26] N. Nernst *et al.* (Crystal Ball Collaboration), Phys. Rev. Lett. **54** (1985) 2195.
- [27] U. Heintz *et al.* (CUSB II Collaboration), Phys. Rev. **D46** (1992) 1928.
- [28] R.A. Briere *et al.* (CLEO Collaboration), Phys. Rev. **D70** (2004) 072001.
- [29] *QQ - The CLEO Event Generator*,  
<http://www.lns.cornell.edu/public/CLEO/soft/QQ> (unpublished).
- [30] R. Brun et al., GEANT 3.21, CERN Program Library Long Writeup W5013 (1993).
- [31] S. Eidelman *et al.*, Review of Particle Physics, Phys. Lett. **B592** (2004) 1.
- [32] X.-G. He, H.-Y. Jin and J.P. Ma, Phys. Rev. **D66** (2002) 074015.